Biochimica et Biophysica Acta 1818 (2012) 33–41

Contents lists available at SciVerse ScienceDirect

Biochimica et Biophysica Acta

journal homepage: www.elsevier.com/locate/bbamem

Identification and functional characterization of zebrafish K_{2P}10.1 (TREK2) two-pore-domain K^+ channels

Jakob Gierten, David Hassel, Patrick A. Schweizer, Rüdiger Becker, Hugo A. Katus, Dierk Thomas *

Department of Cardiology, Medical University Hospital Heidelberg, Im Neuenheimer Feld 410, D-69120 Heidelberg, Germany

ARTICLE INFO

Article history:
Received 29 June 2011
Received in revised form 9 September 2011
Accepted 13 September 2011
Available online 22 September 2011

Keywords:
Electrophysiology
Ion channel
K^+ leak current
K_{2P}10.1 (TREK2)
Membrane potential
Zebrafish

ABSTRACT

Two-pore-domain potassium (K_{2P}) channels mediate K^+ background currents that stabilize the resting membrane potential and contribute to repolarization of action potentials in excitable cells. The functional significance of K_{2P} currents in cardiac electrophysiology remains poorly understood. *Danio rerio* (zebrafish) may be utilized to elucidate the role of cardiac K_{2P} channels in vivo. The aim of this work was to identify and functionally characterize a zebrafish otholog of the human K_{2P}10.1 channel. K_{2P}10.1 orthologs in the *D. rerio* genome were identified by database analysis, and the full zK_{2P}10.1 coding sequence was amplified from zebrafish cDNA. Human and zebrafish K_{2P}10.1 proteins share 61% identity. High degrees of conservation were observed in protein domains relevant for structural integrity and regulation. K_{2P}10.1 channels were heterologously expressed in *Xenopus* oocytes, and currents were recorded using two-electrode voltage clamp electrophysiology. Human and zebrafish channels mediated K^+ selective background currents leading to membrane hyperpolarization. Arachidonic acid, an activator of hK_{2P}10.1, induced robust activation of zK_{2P}10.1. Activity of both channels was reduced by protein kinase C. Similar to its human counterpart, zK_{2P}10.1 was inhibited by the antiarrhythmic drug amiodarone. In summary, zebrafish harbor K_{2P}10.1 two-pore-domain K^+ channels that exhibit structural and functional properties largely similar to human K_{2P}10.1. We conclude that the zebrafish represents a valid model to study K_{2P}10.1 function *in vivo*.

1. Introduction

Two-pore-domain potassium (K_{2P}) channels mediate K^+ background (or "leak") currents that stabilize the negative resting membrane potential (RMP) and contribute to repolarization of action potentials [1]. Tightly regulated leak currents control cellular excitability in the heart and other tissues [1–3]. Owing to their ubiquitous expression, K_{2P} channels are involved in multiple physiological functions including cardioprotection, neuronal plasticity, muscle contraction, and hormone secretion [4]. Repolarization of cardiomyocytes is mediated by different potassium channels [5]. The distinct cardiac plateau current (I_{KP}) is an instantaneously activating, non-inactivating K^+ current that modulates amplitude and duration of the cardiac action potential [6]. Based on common distribution and pharmacological and biophysical properties K_{2P} channels have been suggested as molecular counterparts of I_{KP} [7]. Expression of K_{2P}10.1 (TREK2; TWIK-related K^+ channel 2) has been detected in human, rat, and chicken heart, with predominant expression in atrial cells [8–12]. In chicken, K_{2P}10.1 and the related K_{2P}2.1 (TREK1) channels carry a thermosensitive and arachidonic acid (AA)-activated background current that is responsible for hyperpolarization and stabilization of RMP in embryonic atrial cardiomyocytes [12]. In addition, K_{2P}10.1 has been suggested to contribute to a neuronal background conductance [13] and is implicated in control of neuronal excitability and spatial learning [14]. K_{2P}10.1 activity is enhanced by a wide range of physical and chemical stimuli, including increase in temperature to 37 °C [15], mechanical stretch [13], intra- and extracellular acidification [8,16], bioactive lipids such as polyunsaturated fatty acids (PUFAs) [13] or lysophospholipids [8,17], and volatile anesthetics [8,10]. Stimulation of G protein-coupled membrane receptors by different neurotransmitters and hormones and activation of protein kinase pathways leads to inhibition of K_{2P}10.1 channels [8,10,18,19].

Zebrafish (*Danio rerio*) is an established model for human disease that is widely used in developmental biology [20]. Forward (phenotype-focused) [21] and reverse (candidate gene-centered) [22] genetic approaches render zebrafish a genetically tractable animal model. In addition, this technology offers experimental advantages relative to mammalian systems in drug discovery and safety pharmacology, as zebrafish embryos allow for rapid and high-throughput analysis using whole organism phenotypic assays [23]. Furthermore, zebrafish

Abbreviations: AA, arachidonic acid; aa, amino acids; CDS, coding sequence; E_{rev}, reversal potential; h, human; *I*, current; I_{KP}, cardiac plateau current; ISH, in situ hybridization; K_{2P} channel, two-pore-domain potassium channel; M1 and M2, first and second translation initiation sites; ORF, open reading frame; P, pore domain; PA, palmitic acid; PKC, protein kinase C; PMA, phorbol 12-myristate 13-acetate; PUFA, polyunsaturated acid; r, rat; RMP, resting membrane potential; TASK, TWIK-related acid sensitive K^+ channel; TM, transmembrane domain; TRAAK, TWIK-related arachidonic acid-stimulated K^+ channel; TREK, TWIK-related K^+ channel; TWIK, tandem of P domains in a weak inward rectifying K^+ channel; UTR, untranslated region; *V*, voltage; z, zebrafish

* Corresponding author. Tel.: +49 6221 568855; fax: +49 6221 565514.
E-mail address: dierk.thomas@med.uni-heidelberg.de (D. Thomas).

0005-2736/$ – see front matter © 2011 Elsevier B.V. All rights reserved.
doi:10.1016/j.bbamem.2011.09.015

embryos are transparent and well suited for in vivo imaging studies. Recent studies established zebrafish as genetic and functional model for cardiac electrophysiology [24]. Mutations or pharmacological modulation of the repolarizing zebrafish ether-a-go-go-related gene (zERG/I_{Kr}) potassium channel result in long or short QT syndromes [23,25,26]. Electrophysiological similarities between zebrafish and humans were extended to SCN5A sodium channel subunits, aquaporins, connexin 43, transient receptor potential (TRP) channels, L-type calcium channels, and Kir1.1 inward rectifier channels [27–31]. To date, zebrafish has not been established to elucidate cardiac function of K_{2P}10.1 and other K_{2P} channels. Here we report cloning and functional characterization of zebrafish K_{2P}10.1 two-pore-domain K^+ channels. Human and zebrafish K_{2P}10.1 display similar electrophysiological properties and are sensitive to antiarrhythmic drugs. We conclude that the zebrafish represents an appropriate model to study in vivo function of K_{2P}10.1.

2. Material and methods

2.1. Molecular biology

Potential orthologs of hK_{2P} channels in the *D. rerio* genome were identified by reciprocal BLAST analysis (National Center for Biotechnology Information, Bethesda, USA). Human K_{2P} query sequences were included in TBLASTN search against a zebrafish nucleotide collection (nr/nt). Highest scoring hits were confirmed as potential orthologs if the reciprocal BLASTX screen recognized the initial hK_{2P} protein in non-redundant protein sequence database (nr). TBLASTN search using human K_{2P}10.1 isoform 2 (GenBank accession number NP_612190.1) as query sequence yielded two hits with high alignment scores (E-value $\leq 4e^{-162}$). Both hits represent nucleotide sequences of z*KCNK*10 genes. The first mRNA target (XM_686592.3) is encoded by the z*KCNK*10a gene on zebrafish chromosome 20, as assigned by Ensembl genome browser (Ensembl, HAVANA group, Welcome Trust Sanger Institute, Hinxton, UK). The second mRNA hit (XM_688902.2) is linked to the z*KCNK*10b gene on chromosome 17. Reciprocal BLASTX for z*KCNK*10a mRNA (XM_686592.3) and z*KCNK*10b mRNA (XM_688902.2) yielded hK_{2P}10.1 isoforms 1–3 as matching targets (E-values $\leq 8e^{-174}$), supporting z*KCNK*10a and z*KCNK*10b as putative orthologs to human *KCNK*10.

Our primary aim was to establish functional similarity between human and zebrafish K_{2P} channel orthologs, serving as proof-of-concept. Zebrafish K_{2P}10.1b produces an isoform with similar size compared to the protein length of three human K_{2P}10.1 isoforms. This study confirmed expression and function of zebrafish z*KCNK*10b channels, and extension to *KCNK*10a was not required. The entire open reading frame (ORF) of z*KCNK*10b was amplified in this work. Cloning primer sequences located in the proposed untranslated regions (UTR) were derived from the genomic sequence using automated and manually annotated transcript structures of z*KCNK*10b (Ensembl). The first hypothetical translation initiation site (M1) (TCGGCCATGC) annotated by Ensembl and vertebrate genome annotation (Vega; Welcome Trust Sanger Institute) databases has only a suboptimal Kozak context [32]. Thus, forward primers were designed to include a start codon with a strong Kozak sequence corresponding to the human clone that was identified 59 bases upstream. Reverse primers were situated within the proposed 3′-UTR between the translational stop sequence and a consensus sequence for polyadenlyation [33] 609 bases downstream. The entire coding sequence (CDS) of z*KCNK*10b corresponding to sequence XM_688902.2 was amplified by nested PCR from adult zebrafish cDNA using two sets of forward and reverse primers, respectively (F1, 5′-GCACATTTCAGAGCACTTTGTGAGACC-3′; R1, 5′-GCATTTAAAGCTCTCTCAGCCTCTTTATGAAAC-3′; F2, 5′-CCACCCAGTTCTGATCATCTCCGTCTC-3′; R2, 5′-GAATTTGGCCCTTCAGGTGTGATCG-3′). Resulting DNA was cloned into pCR2.1-TOPO (Invitrogen, Karlsruhe, Germany). The final z*KCNK*10b insert was amplified from pCR2.1-TOPO (F3, 5′-CACGACCTGGTCGACCAGACCAACATGGTCCCGCAG-3′; R3, 5′-GTGGTAACCAGATCTTTACTACGGTTGGTGTTCCTTCAGCTCCAG-3′) and subcloned into pRAT, a dual-purpose expression vector containing a CMV promoter for mammalian expression and a T7 promoter for cRNA synthesis. pCR2.1-TOPO and pRAT-z*KCNK*10 clones were sequenced.

For *in vitro* transcription, pRAT-z*KCNK*10b (FJ888634.1) was linearized with *Not*I and transcribed using T7 RNA polymerase and the mMessage mMachine kit (Ambion, Austin, USA). Transcripts and control samples were separated by agarose gel electrophoresis and quantified by spectrophotometry. For heterologous expression 46 nl of cRNA were injected into stage V–VI defolliculated *Xenopus* oocytes and incubated for 2 to 3 days at 18 °C. This study has been carried out in accordance with the Council Directive 86/609/EEC on the protection of animals used for scientific purposes released by the European Commission.

2.2. In situ hybridization

A digoxigenin-labeled z*KCNK*10b antisense probe (607 bases) was synthesized using T7 polymerase from z*KCNK*10b in pCR2.1-TOPO vector linearized with SgrAI as template. Whole-mount in situ antisense RNA hybridization (ISH) was carried out as described [34,35].

2.3. Electrophysiology

Whole cell currents were measured by two-electrode voltage clamp as published previously [36]. Briefly, currents were recorded with an Oocyte Clamp amplifier (Warner Instruments, Hamden, USA) using pCLAMP (Axon Instruments, Foster City, USA) and Origin (OriginLab, Northampton, USA) software for data acquisition and analysis. Data were sampled at 2 kHz, filtered at 1 kHz. Current amplitudes were determined at the end of + 60 mV pulses. No leak current subtraction was performed. Two-electrode voltage clamp electrode pipettes were produced from glass capillary tubes GB100F-10 (Science Products, Hofheim, Germany) using a P-87 micropipette puller (Sutter Instruments, Novato, USA). Pipettes were filled with 3 M KCL and had a tip resistance of 1–5 MΩ. All experiments were conducted at room temperature (20–22 °C).

2.4. Solutions and drug administration

The standard physiological extracellular solution contained 96 mM NaCl, 4 mM KCl, 1.1 mM $CaCl_2$, 1 mM $MgCl_2$, 5 mM HEPES and was adjusted to pH 7.4 with NaOH. Stock solutions of arachidonic acid (AA; 20 mM), palmitic acid (PA; 100 mM), quinidine (100 mM), and amiodarone (10 mM; all agents obtained from Sigma-Aldrich, Steinheim, Germany) were prepared in ethanol. Phorbol 12-myristate 13-acetate (PMA; Sigma-Aldrich) and Ro-32-0432 (Calbiochem, Darmstadt, Germany) were reconstituted in DMSO to stock solutions of 10 mM. $ZnCl_2$ (Sigma-Aldrich) was dissolved in standard extracellular solution (100 mM). Aliquots of stock solutions were stored at − 20 °C and diluted to desired concentrations in the standard extracellular solution on the day of experiment. Baseline currents were measured before drug administration, and drug effects on channel activity were assessed following incubation periods of 30 min (PMA), 3 h (AA, PA, quinidine, amiodarone), and 4 h (Ro-32-0432). Corresponding control periods of 30 min, 3 h, and 4 h in standard extracellular solution had no significant effects on hK_{2P}10.1 or zK_{2P}10.1 currents ($n = 5–28$; data not shown). Application of 100 μM Zn^{2+} (30 min) activated endogenous currents by 4.68 ± 1.15-fold ($n = 5$; $p = 0.026$). This affect, however, did not significantly affect the assessment of K_{2P}10.1 regulation, as endogenous currents after application of Zn^{2+} constituted a negligible fraction of outward currents in the presence of heterologously expressed hK_{2P}10.1 and zK_{2P}10.1 currents (3.1% and 12.9%, respectively). The remaining agents used in this work were tested on mock (0.1 M KCl) injected cells as well, excluding

effects on endogenous *Xenopus* currents (n = 4–13; data not shown). Finally, solvents were applied at maximum bath concentrations to assess potential unspecific effects. Incubation in 1% ethanol solution for 3 h had no effect on $hK_{2P}10.1$ currents and on mock-injected cells (n = 7–8 cells; data not shown), while $zK_{2P}10.1$ currents displayed weak activation (1.2 ± 0.03-fold; n = 6; p = 0.004). Application of 0.03% DMSO for 4 h did not significantly affect $hK_{2P}10.1$ and $zK_{2P}10.1$ channels or mock-injected cells (n = 6–9; data not shown).

2.5. Data analysis and statistics

Data are expressed as mean ± standard error of the mean (SEM). We used paired and unpaired Student's *t* tests (two-tailed tests) to compare the statistical significance of the results. $P<0.05$ was considered statistically significant. Preparation and formatting of the manuscript were performed in accordance with Uniform Requirements for Manuscripts Submitted to Biomedical Journals promulgated by the International Committee of Medical Journal Editors.

3. Results

3.1. Phylogenetic relation of zebrafish and human K_{2P} channels

Zebrafish orthologs of human K_{2P} channels were identified by Ensembl predictions or using reciprocal BLAST searches (Fig. 1). Jukes–Cantor genetic distance model and the neighbor-joining tree build method were used to assemble phylogenetic trees. Putative paralogous gene pairs (i.e., related genes originating from duplication of a single ancestral gene within a genome) were available for z*KCNK*1, z*KCNK*2, z*KCNK*3, z*KCNK*5, z*KCNK*10, and z*KCNK*13 (Fig. 1). No sequence prediction or BLAST result was found for *KCNK*16. The presence of two gene copies reflects a genome duplication event in zebrafish at the base of teleost radiation [37]. Using the *Drosophila melanogaster* K_{2P} channel ORK1 [38] as an outgroup indicated that zebrafish K_{2P} channels are closer related to human K_{2P} channels compared to *Drosophila*.

3.2. Cloning of zKCNK10b

Database search for orthologs of $hK_{2P}10.1$ channel revealed two target sequences (GenBank accession numbers XM_686592.3 and XM_688902.2) representing mRNA predictions for $zK_{2P}10.1$. Both hits refer to *KCNK*10 genes in the zebrafish genome. Predicted $K_{2P}10.1$ orthologs are encoded by z*KCNK*10a (chromosome 20) and z*KCNK*10b (chromosome 17) genes. Each z*KCNK*10 gene is predicted to produce a single isoform. A transcript encoding for 569 amino acids (aa) is suggested for the z*KCNK*10a gene. In contrast, software-based automatic database analyses predicted that z*KCNK*10b produces an isoform of at least 528 aa that correlates reasonably well with the protein length of three human $K_{2P}10.1$ isoforms (isoform 1, 538 aa; isoform 2, 543 aa; isoform 3, 543 aa). However, the software-annotated hypothetical $zK_{2P}10.1$ sequence was incomplete, lacking an upstream start codon with a strong Kozak sequence corresponding to the human isoform 2 clone. Annotation of the upstream AUG corresponds to GenBank sequence XM_688902.2. Thus, the resulting full coding sequence of z*KCNK*10b (551 aa) was amplified in this work by nested PCR.

3.3. Genomic organization of zKCNK10b and hKCNK10

The genomic sequence of z*KCNK*10b on chromosome 17 comprises 31593 base pairs (bp) (Fig. 2A). N terminus and transmembrane

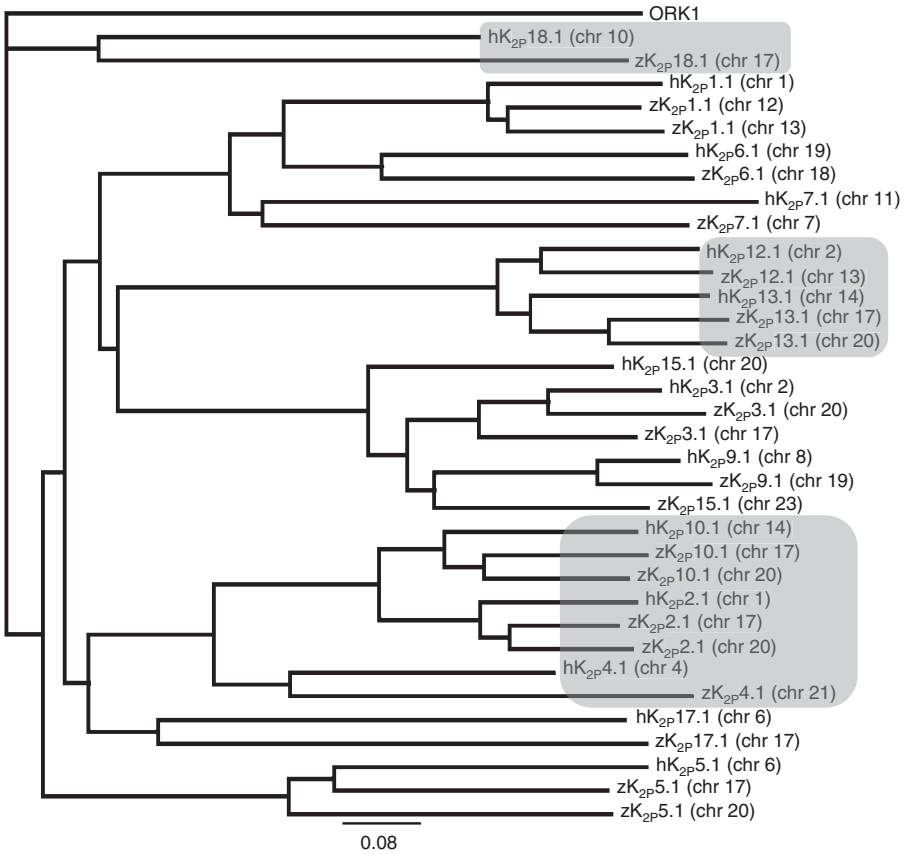

Fig. 1. Phylogram of human, zebrafish, and *Drosophila* K_{2P} channels. Predicted zK_{2P} protein sequences were aligned to respective human orthologs and assembled in a phylogenetic tree view. Zebrafish $K_{2P}1.1$, $K_{2P}2.1$, $K_{2P}3.1$, $K_{2P}5.1$, $K_{2P}10.1$, and $K_{2P}13.1$ show gene duplications (paralogs). Human and zebrafish K_{2P} channels may be subdivided into functional classes, indicated by gray panels. The scale bar represents the average number of amino acid substitutions per site.

domain (TM) 1 are encoded by a single exon 1 in zebrafish, while corresponding segments in human $K_{2P}10.1$ are encoded by two exons. The remaining exon structure is similar in both species. Alternative usage of $hK_{2P}10.1$ exon 1 produces three isoforms that differ in their N-terminal domains [10]. Furthermore, alternative mRNA translation initiation (ATI) regulates expression and electrophysiological function of human $K_{2P}10.1$ channels [39,40]. Human $K_{2P}10.1$ channels harbor three alternative translation initiation sites [39,40]. In contrast, analysis of the $zK_{2P}10.1$ N terminus revealed five AUG codons that may serve as alternative start sites for ribosomal translation. The functional significance of putative ATI sites in zebrafish $K_{2P}10.1$ remains to be elucidated. Human $K_{2P}10.1$ isoform 2 (IF2) has been detected in the heart and displays a translation initiation nucleotide context similar to zebrafish $K_{2P}10.1$. Thus, $zK_{2P}10.1$ was compared with $hK_{2P}10.1$ isoform 2 in functional analyses.

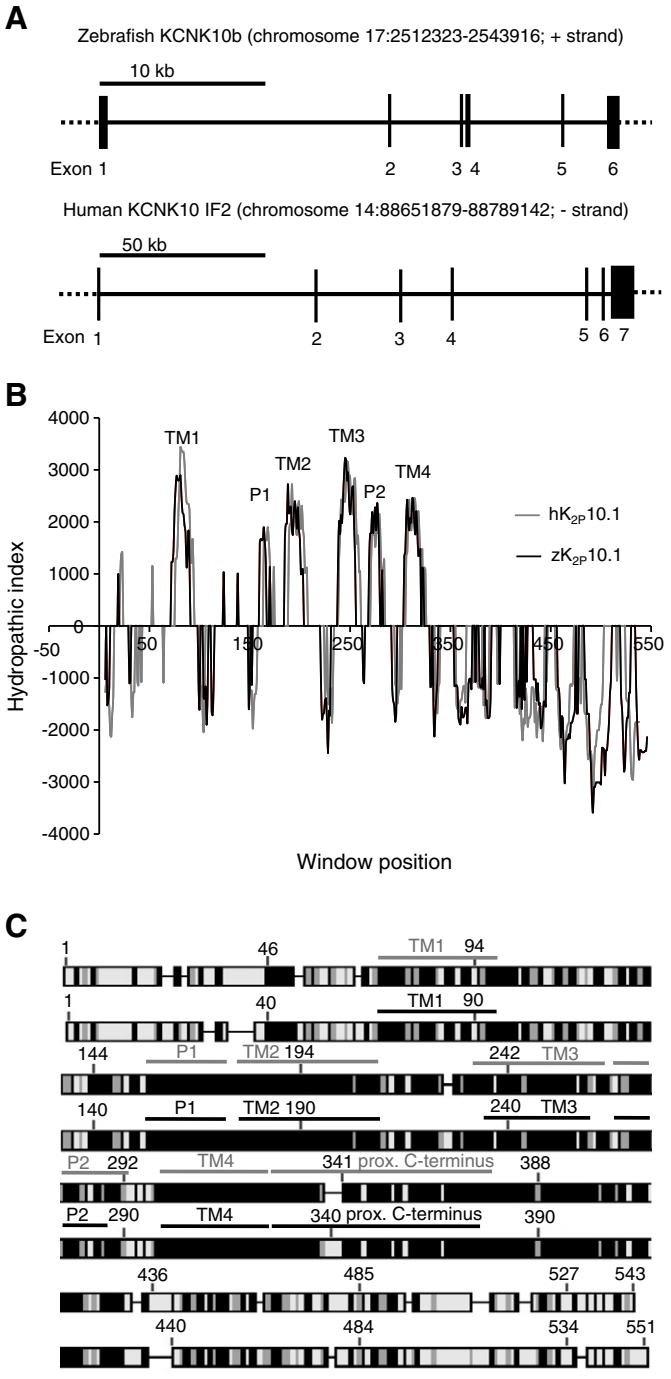

Fig. 2. Genetic and biochemical similarities between zebrafish and human $K_{2P}10.1$. (A) Genomic organization of z*KCNK*10b and h*KCNK*10. (B) Hydrophobicitiy analysis (Kyte and Doolittle scale) of $K_{2P}10.1$ polypeptides, revealing predicted 4 TM (transmembrane domain)/2 P (pore domain)-topologies. (C) Protein alignment of human and $zK_{2P}10.1$ polypeptides, showing conservation of functional relevant transmembrane, pore, and proximal C-terminal domains. Numbers indicate amino acid positions. Identical and similar amino acids are represented by black and gray color, respectively. White color indicates no similarity.

3.4. Molecular structure of $zK_{2P}10.1$

Cloned zebrafish *KCNK*10b encodes a 551 aa polypeptide with a calculated mass of 61.5 kDa and harbors typical domains of mammalian K_{2P} channels. Hydropathy analysis of the protein sequence identified four transmembrane domains (TM) with intracellular N and C termini (Fig. 2B). A large loop connects TM1 with the first pore domain (P1), as described previously for $K_{2P}2.1$, $K_{2P}10.1$, and $K_{2P}4.1$ (TRAAK; TWIK-related arachidonic acid-stimulated K^+ channel) channels [8,41]. The $zK_{2P}10.1$ TM1-P1-loop contains a cysteine residue (C119) corresponding to C123 in human $K_{2P}10.1$ and to C69 in $hK_{2P}1.1$ (TWIK1; tandem of P domains in a weak inward rectifying K^+ channel 1) that is involved in $hK_{2P}1.1$ homodimerization via disulfide bonds [42]. The second P domain is located between TM3 and TM4. Comparison of the transmembrane structure of $zK_{2P}10.1$ and $hK_{2P}10.1$ revealed a significant match between both sequences (Fig. 2B). Proteins were aligned using BLOSUM50 as similarity matrix and gap open and gap extension penalties of 10 and 2, respectively. Protein alignment showed 61% identify and high similarities in TM, P, and proximal C-terminal domains. In contrast, the N terminus and the distal C-terminal sequence of $zK_{2P}10.1$ deviate from the corresponding segments in $hK_{2P}10.1$ (Fig. 2C, Supplementary material).

In rat (r), $K_{2P}10.1$ channel activity is decreased by protein kinase C (PKC)-dependent phosphorylation at serine residues 326 and 359 [19]. Both sites are conserved in human (S331, S364) and zebrafish (S329, S366) subunits. The proximal C terminus (~the first 50 C-terminal aa) of $rK_{2P}10.1$ is crucial for channel opening [43]. This sequence is identical to $hK_{2P}10.1$ (R328-I377) and displays 75% identity with the proximal C terminus of $zK_{2P}10.1$, while distal C termini of human and zebrafish $K_{2P}10.1$ share only 38% homology. Furthermore, polyunsaturated fatty acids (PUFAs) are strong activators of $K_{2P}10.1$ [44]. Zebrafish $K_{2P}10.1$ bears a positively charged sequence (KKTKEE) closely following TM4 that is conserved in rat and human $K_{2P}10.1$ which has been proposed as critical structural element for fatty acid sensitivity [43]. Significant structural homologies between human and zebrafish $K_{2P}10.1$ proteins suggest similar functional regulation.

3.5. $K_{2P}10.1$ tissue distribution

Tissue distribution of *KCNK*10b transcripts was assessed by antisense RNA whole-mount in situ staining (Fig. 3). We observed $K_{2P}10.1$ to be ubiquitously expressed in zebrafish embryos at 72 h after fertilization (Fig. 3A). Pronounced expression of $K_{2P}10.1$ RNA was detected in the brain, eye, heart, notochord, and myosepts (Fig. 3B).

3.6. Functional expression of $zK_{2P}10.1$ channels

Functional properties of $K_{2P}10.1$ channels were studied in *Xenopus laevis* oocytes. From a holding potential of −80 mV, depolarizing pulses were applied for 500 ms to voltages between −140 and +60 mV in 20 mV increments (0.5 Hz). Oocytes injected with z*KCNK*10b or h*KCNK*10 cRNA showed non-inactivating outward currents upon depolarization that were not observed in mock-injected cells (Fig. 4A, B). Zebrafish $K_{2P}10.1$ currents exhibited instantaneous activation, whereas human $K_{2P}10.1$ channels activated in two phases. First, ~75% of their respective maximum amplitudes was quickly established, followed by markedly slower additional activation time

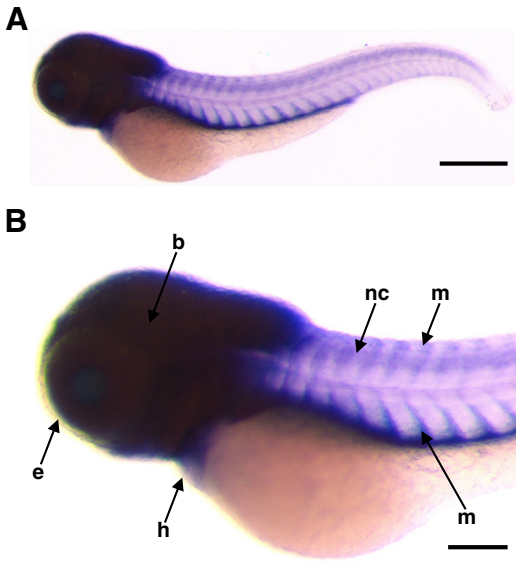

Fig. 3. Whole-mount antisense RNA in situ hybridization of zebrafish *KCNK*10b expression. (A, B) Lateral views of zebrafish embryos 72 h after fertilization. Scale bars, 500 μm (A) and 200 μm (B). Purple staining indicates expression in brain (b), eye (e), heart (h), notochord (nc), and myosepts (m).

course (Fig. 4A). In physiological low K^+ solution, $zK_{2P}10.1$ mediated outwardly rectifying currents that shifted the reversal potential (E_{rev}) toward hyperpolarized values (-50.6 ± 2.1 mV; n = 5) compared to mock injected cells ($E_{rev} = -20.2 \pm 1.1$ mV; n = 5) (Fig. 4B). The normalized current–voltage (*I–V*) relation of $K_{2P}10.1$ currents was similar between species (Fig. 4C).

To assess ion selectivity of $zK_{2P}10.1$, external K^+ was elevated from 4 mM to 20 mM and 100 mM, respectively. Both $hK_{2P}10.1$ and $zK_{2P}10.1$ passed larger outward currents at low K^+ (Fig. 5A, B). In contrast, high external K^+ led to increased inward currents at negative potentials and to linear *I–V* relationships, as expected for K^+ selective ion channels (Fig. 5A, B). In addition, $zK_{2P}10.1$ and $hK_{2P}10.1$ resting membrane potentials were depolarized as the electrochemical driving force for hyperpolarizing K^+ currents is decreased at elevated external K^+ levels (Fig. 5C, D). External K^+ concentration plotted against the respective reversal potentials displayed slopes of 36.1 ± 0.9 mV ($hK_{2P}10.1$; n = 5) and 28.9 ± 0.5 mV ($zK_{2P}10.1$; n = 5) per 5-fold change in $[K^+]_e$ (Fig. 5A, B), indicating similar K^+ selectivity of the channels. The reversal potential of a membrane solely selective for K^+ ions corresponds to the Nernst equilibrium potential for K^+ (E_K). A 5-fold increase of $[K^+]_e$ induces a calculated depolarization of E_K by 41 mV at 21 °C with $[K^+]_i = 150$ mM. In our experimental setting we observed smaller shifts in oocytes expressing $hK_{2P}10.1$ or $zK_{2P}10.1$ per 5-fold change in $[K^+]_e$, possibly caused by leak of other positively charged ions (e.g. Na^+, Ca^{2+}).

3.7. Zebrafish and human $K_{2P}10.1$ channels exhibit similar sensitivity to activators and inhibitors

Activation by polyunsaturated fatty acids is a key feature of $K_{2P}10.1$ currents. Zebrafish $K_{2P}10.1$ bears a positive cluster sequence KKTKEE in the proximal C terminus that has been described as a

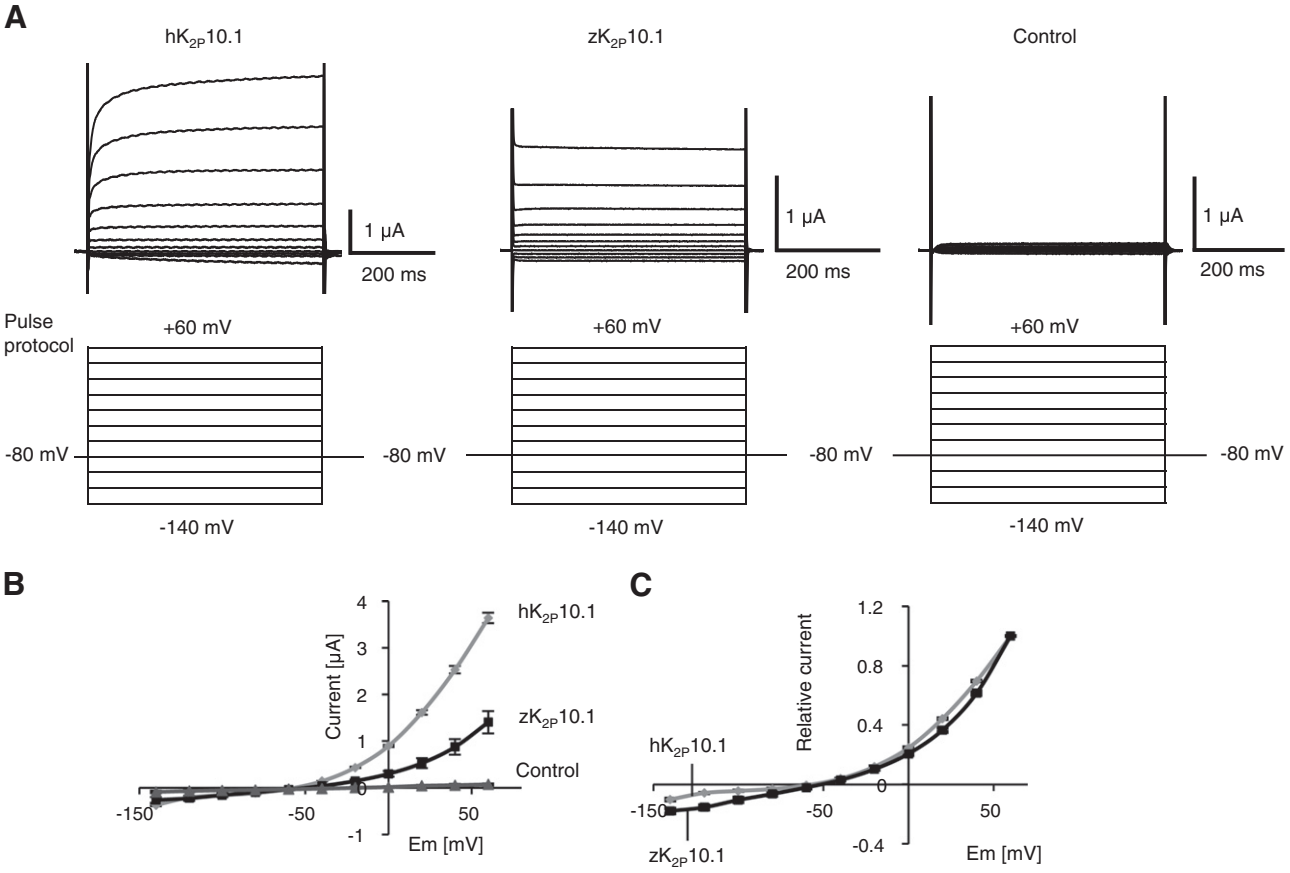

Fig. 4. Functional expression of $zK_{2P}10.1$ and $hK_{2P}10.1$ in *Xenopus* oocytes. (A) Depolarization of cell membranes elicited outward currents in representative cells expressing $hK_{2P}10.1$ or $zK_{2P}10.1$. Control oocytes did not exhibit significant K^+ currents. Panels (B) and (C) display activation curves, i.e. step current amplitudes as function of test potentials, recorded under isochronal conditions (B, original current amplitudes; C, values normalized to maximum currents) (n = 5 cells each). Error bars denote SEM. In physiological salt solution (low external K^+), $K_{2P}10.1$ currents showed outward rectification. (C) Normalization of h/$zK_{2P}10.1$ currents revealed similar voltage-dependence of activation.

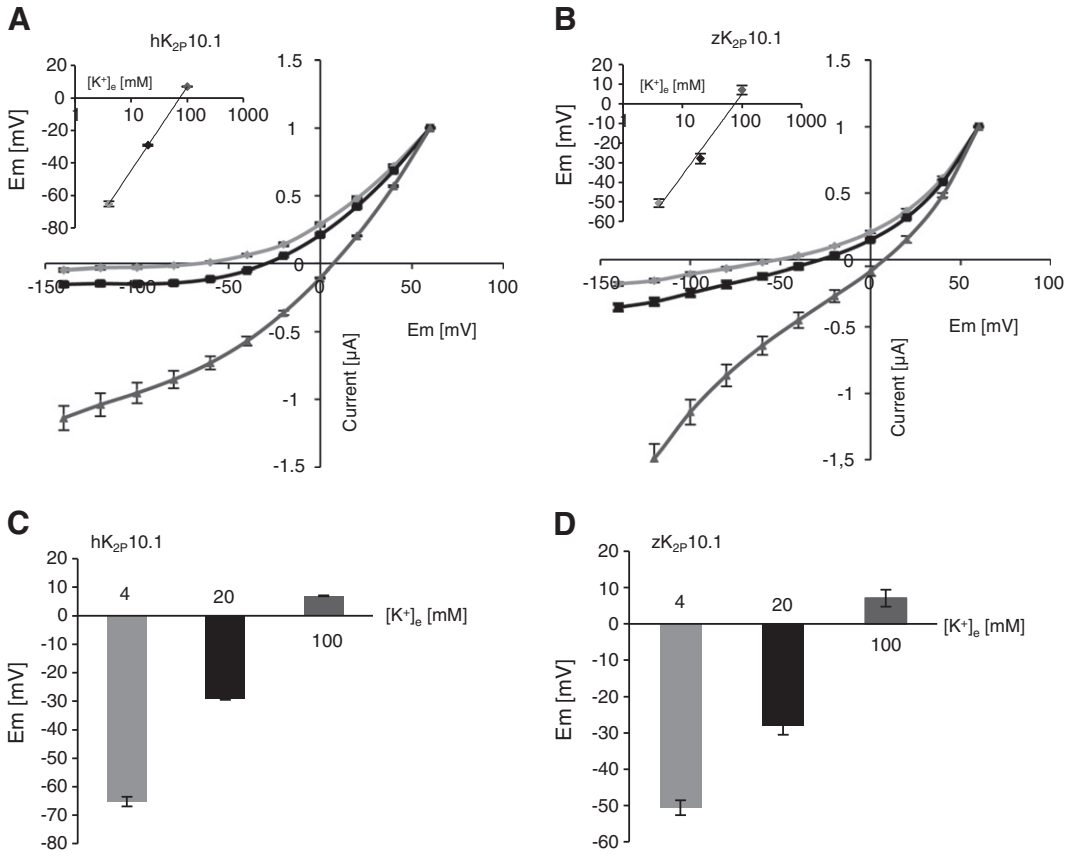

Fig. 5. Ion selectivity of $zK_{2P}10.1$ and $hK_{2P}10.1$ channels. (A, B) Titration of extracellular potassium concentrations from 4 mM to 100 mM induced rightward shifts and virtual linearization of $hK_{2P}10.1$ (A) and $zK_{2P}10.1$ (B) activation curves (n = 5). (C, D) K^+-dependent resting membrane potential depolarization demonstrates K^+ selectivity of $K_{2P}10.1$ background channels. Insets in panels A and B, Relationships between membrane potentials and K^+ concentrations indicate selectivity for K^+. Data are given as mean ± SEM.

crucial element for fatty acid sensitivity in mammalian channels [43]. Thus, we tested whether arachidonic acid (AA) could stimulate whole-cell currents (Fig. 6A). Treatment with 20 µM AA for 3 h increased channel activity by 3.6 ± 0.3-fold compared to respective baseline currents (n = 13; p < 0.0001). A similar stimulating effect of AA was observed for human $K_{2P}10.1$ (3.5 ± 0.1-fold increase; n = 5; p = 0.0001). Saturated palmitic acid (PA) served as negative control (100 µM; 3 h) and did not significantly modulate $hK_{2P}10.1$ currents, whereas $zK_{2P}10.1$ exhibited moderate activation upon exposure to PA (1.2 ± 0.1-fold increase; n = 11; p = 0.017).

The *zKCNK*10 sequence harbors two putative PKC sites. Therefore we assessed whether modulation of PKC activation would alter $zK_{2P}10.1$ channel activity in comparison to $hK_{2P}10.1$ (Fig. 6B, C). Whole-cell $K_{2P}10.1$ currents determined after treatment with the PKC activator PMA (100 nM; 30 min) were significantly reduced, with a predominant effect on $hK_{2P}10.1$ ($I_{zK2P10.1}$, −24.3 ± 3.3%; n = 7; p = 0.0009; $I_{hK2P10.1}$, −80.9 ± 2.15%; n = 8; p = 0.0018). PMA effects on $hK_{2P}10.1$ and $zK_{2P}10.1$ were significantly different (p < 0.0001) (Fig. 6B). Conversely, suppression of PKC activity by Ro-32-0432 (3 µM; 4 h) produced weak $K_{2P}10.1$ channel activation ($I_{zK2P10.1}$, +20.9 ± 6.2%; n = 12; p = 0.020; $I_{hK2P10.1}$, +6.4 ± 2.5%; n = 9; p = 0.041) (Fig. 6C).

Antiarrhythmic drug sensitivity of $K_{2P}10.1$ was evaluated using quinidine and amiodarone. Treatment of zebrafish and human $K_{2P}10.1$ with 100 µM quinidine for 3 h resulted in current reduction that did not reach statistical significance ($I_{zK2P10.1}$, −9.6 ± 6.7%; n = 9; p = 0.077; $I_{hK2P10.1}$, −20.7 ± 3.5%; n = 9; p = 0.052) (Fig. 6D). In contrast, amiodarone (100 µM; 3 h) which has been reported to inhibit $hK_{2P}3.1$ channels [45] significantly decreased $K_{2P}10.1$ currents ($I_{zK2P10.1}$, −34.9 ± 1.2%; n = 6; p = 0.0001; $I_{hK2P10.1}$, −41.6 ± 4.5%; n = 4; p = 0.022) (Fig. 6E).

Selective modulation of ion channel activity represents a valuable approach to study the specific physiological impact of a particular ionic current. Zn^{2+} has been identified as selective activator of $K_{2P}10.1$ (TREK2), while $K_{2P}2.1$ (TREK1) current is inhibited and $K_{2P}3.1$ (TASK1) or $K_{2P}5.1$ (TASK2) are not affected [46–48]. To study the effect of Zn^{2+} on study channels, voltage ramp pulses were applied between −140 and +60 mV (500 ms), indicating activation of zebrafish and human $K_{2P}10.1$ currents following application of 100 µM Zn^{2+} for 30 min (Fig. 7A). Current increase (100 µM Zn^{2+}; 30 min) was quantified using the protocol described in Fig. 4, revealing 2.27 ± 0.18-fold ($hK_{2P}10.1$; n = 9; p = 0.0003) and 3.64 ± 0.46-fold current increase ($zK_{2P}10.1$; n = 12; p = 0.0049), respectively (Fig. 7B). Response of $zK_{2P}10.1$ channels to Zn^{2+} treatment was significantly stronger compared to $hK_{2P}10.1$ (p = 0.024).

4. Discussion

We report cloning of a zebrafish ortholog of human $K_{2P}10.1$ (TREK2) background channels. Comparison of biophysical and pharmacological properties revealed similar function and regulation of $zK_{2P}10.1$ and $hK_{2P}10.1$.

4.1. The zebrafish KCNK gene family

The *D. rerio* genome contains two copies of the *KCNK*10 gene that are mapped to chromosome 20 (z*KCNK*10a) and chromosome 17 (z*KCNK*10b), respectively, whereas a single *KCNK*10 gene is present on chromosome 14 in humans. The disproportion between zebrafish and human *KCNK*10 gene numbers is applicable to other K_{2P} channel genes as well (z*KCNK*1, z*KCNK*2, z*KCNK*3, z*KCNK*5, z*KCNK*10, and z*KCNK*13) (Fig. 1). Multiple single mammalian genes correspond to

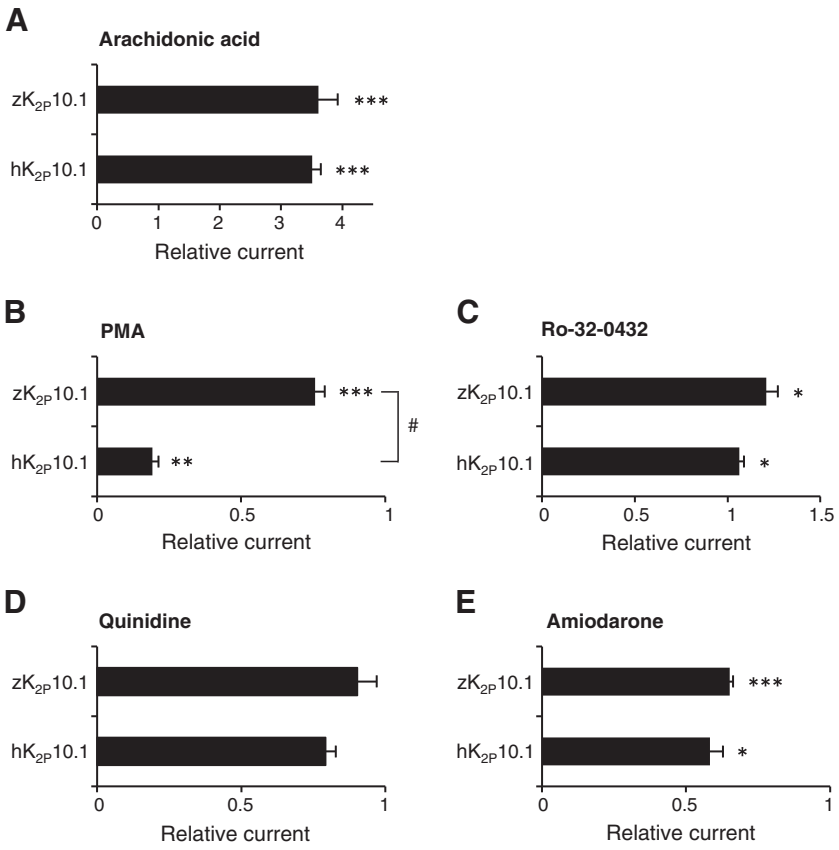

Fig. 6. Regulation of $zK_{2P}10.1$ currents. Relative $hK_{2P}10.1$ and $zK_{2P}10.1$ current amplitudes were determined after treatment with 20 μM arachidonic acid (A), 100 nM PMA (B), 3 μM Ro-32-0432 (C), 100 μM quinidine (D), or 100 μM amiodarone (E) to compare channel sensitivity. Data are provided as mean ± SEM. *$p<0.05$; **$p<0.01$; ***$p<0.001$ versus respective controls. #$p<0.05$ versus human $K_{2P}10.1$.

a pair of respective duplicated zebrafish genes on a genome-wide scale. Evidence from comparative genomics suggests that whole-genome duplication occurred at the base of the teleost lineage following divergence from the tetrapod lineage [49,50]. Only a subset of these duplicates (~20%) is retained in zebrafish [51]. Deletion of most fish-specific duplicates may explain that only single copies were found for z*KCNK*4, z*KCNK*6, z*KCNK*7, z*KCNK*9, z*KCNK*12, z*KCNK*15, z*KCNK*17, and z*KCNK*18 genes (Fig. 1). Furthermore, no zebrafish ortholog of human *KCNK*16 was identified, possibly due to incomplete genome annotation. Comparative analyses of orthologous genes revealed synteny (i.e., the localization of two or more orthologous gene pairs in a conserved gene order on a single chromosome in two different species) between human and zebrafish genomes [52,53]. High syntenic correspondence was found between human chromosome 14 (h*KCNK*10) and zebrafish chromosomes 17 (z*KCNK*10b) and 20 (z*KCNK*10a) [53], supporting the notion that both z*KCNK*10 genes represent duplicated orthologs of h*KCNK*10.

4.2. $zK_{2P}10.1$ mediates potassium-selective background currents

In zebrafish, $K_{2P}10.1$ expression was detected in brain, eye, heart, notochord, and myosepts (Fig. 3). Functional properties of cloned $zK_{2P}10.1$ channels were studied in *Xenopus* oocytes. In physiological salt solution (low K^+), $zK_{2P}10.1$ mediated instantaneously activating, outwardly rectifying currents that did not inactivate, leading to hyperpolarization of the cell membrane comparable to $hK_{2P}10.1$ (Fig. 4). Macroscopic current amplitudes were lower in zebrafish (Fig. 4), however, both channels exhibited similar current–voltage relationships. Augmentation of extracellular K^+ concentration led to increased inward currents at negative potentials and to an *I–V* relation approximating a linear function (Fig. 5). Increased inward currents at high external K^+ levels shifted the *I–V* curve toward more depolarized potentials, reflecting cell membrane depolarization (Fig. 5). Selectivity for potassium ions was further confirmed by systematic reversal potential analysis in solutions with different external K^+ concentrations. In summary, these findings suggest that $zK_{2P}10.1$ subunits form K^+ selective channels in the plasma membrane with similar biophysical properties to $hK_{2P}10.1$. Current rectification depended on transmembrane K^+ distribution and on voltage gradients. This "open rectification" behavior renders $zK_{2P}10.1$ a potential component of I_{KP} [6] in zebrafish cardiomyocytes.

4.3. Pharmacology of $zK_{2P}10.1$ channels

$K_{2P}10.1$ channels are sensitive to polyunsaturated fatty acids [8,13]. Here, arachidonic acid (AA) significantly enhanced human and zebrafish $K_{2P}10.1$ currents (Fig. 6). In contrast, stimulation of Gq-coupled receptors or direct pharmacological activation of PKC have been reported to decrease $K_{2P}10.1$ channel activity [8,10,13,19]. We observed significant $K_{2P}10.1$ current inhibition upon protein kinase C activation using PMA (Fig. 6). Conversely, inhibition of PKC (Ro-32-0432) resulted in current increase, as expected. This regulatory feature was conserved between species.

Regulation of cardiac K_{2P} channels by antiarrhythmic drugs (e.g. amiodarone, carvedilol) is increasingly recognized [45,54], suggesting therapeutic significance in the treatment of heart rhythm disorders. Thus, effects of prototype class I (quinidine) and class III (amiodarone) antiarrhythmic drugs were evaluated. Human and zebrafish $K_{2P}10.1$ currents were significantly reduced by amiodarone (Fig. 6), whereas current reduction by quinidine was not statistically significant. In vivo application of quinidine or amiodarone induced bradycardia in zebrafish [55]. This effect has primarily been attributed to inhibition of the repolarizing cardiac I_{Kr} current carried by ether-a-

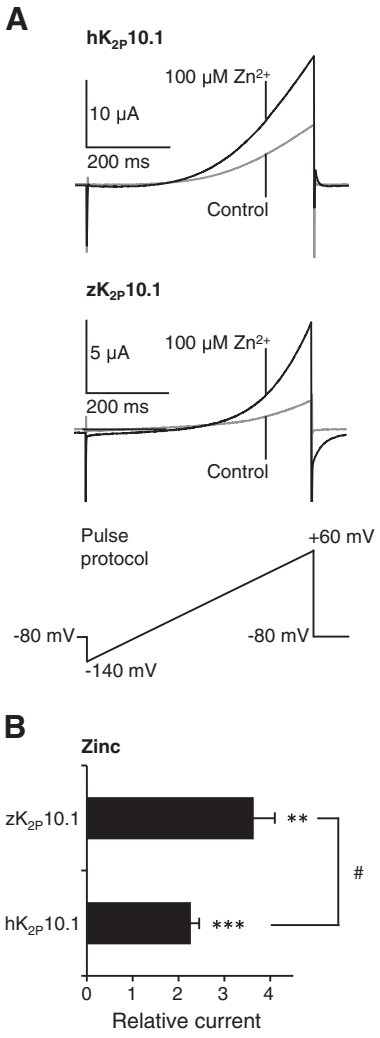

Fig. 7. Activation of $K_{2P}10.1$ channels by Zn^{2+}. (A) Typical current traces before and after Zn^{2+} treatment. Voltage ramps were applied between −140 and +60 mV. (B) Mean (±SEM) relative activation of $hK_{2P}10.1$ and $zK_{2P}10.1$ currents after application of 100 µM Zn^{2+}. **p<0.01; ***p<0.001 versus respective controls; #p<0.05 versus human $K_{2P}10.1$.

go-go-related gene K^+ channels (zERG) [55]. We hypothesize that inhibition of $zK_{2P}10.1$ by amiodarone may contribute to bradycardia in this animal model.

Selective modulation of $K_{2P}10.1$ channels is required to isolate the current in a native environment. Among cardiac K_{2P} channels, divalent Zn^{2+} ions activate $hK_{2P}10.1$, whereas cardiac $hK_{2P}2.1$, $hK_{2P}3.1$, and $hK_{2P}5.1$ channels are blocked or not affected by Zn^{2+} [46–48]. Zn^{2+}-induced $zK_{2P}10.1$ current activation is similar to its human ortholog (Fig. 7). Thus, Zn^{2+} may serve to isolate $K_{2P}10.1$ in zebrafish.

4.4. Conclusion

Zebrafish $K_{2P}10.1$ two-pore-domain channels were identified, cloned, and functionally characterized as potassium-selective open rectifiers similar to their human orthologs. Human and zebrafish $K_{2P}10.1$ channels shared regulation by physiological activators and inhibitors. Furthermore, $K_{2P}10.1$ orthologs were sensitive to antiarrhythmic drugs. Given the similarities between human and zebrafish $K_{2P}10.1$ channels described in this work, we conclude that zebrafish represents a valuable animal model to study the physiological significance of cardiac $K_{2P}10.1$ currents *in vivo*.

Acknowledgements

We thank Ramona Bloehs, Jennifer Gütermann, and Bianca Menrath for their excellent technical assistance. This study was supported in part by research grants from the Deutsche Forschungsgemeinschaft (FRONTIERS program to DT), the ADUMED foundation (to DT), the German Heart Foundation/German Foundation of Heart Research (to DT), and the Max-Planck-Society (TANDEM project to PAS). JG is a fellow of the MD/PhD program at the University of Heidelberg.

Appendix A. Supplementary data

Supplementary data to this article can be found online at doi:10.1016/j.bbamem.2011.09.015.

References

[1] S.A. Goldstein, D. Bockenhauer, I. O'Kelly, N. Zilberberg, Potassium leak channels and the KCNK family of two-P-domain subunits, Nat. Rev. Neurosci. 2 (2001) 175–184.
[2] N.P. Franks, E. Honore, The TREK K_{2P} channels and their role in general anaesthesia and neuroprotection, Trends Pharmacol. Sci. 25 (2004) 601–608.
[3] D.A. Bayliss, P.Q. Barrett, Emerging roles for two-pore-domain potassium channels and their potential therapeutic impact, Trends Pharmacol. Sci. 29 (2008) 566–575.
[4] P. Enyedi, G. Czirjak, Molecular background of leak K^+ currents: two-pore domain potassium channels, Physiol. Rev. 90 (2010) 559–605.
[5] J.M. Nerbonne, R.S. Kass, Molecular physiology of cardiac repolarization, Physiol. Rev. 85 (2005) 1205–1253.
[6] P.H. Backx, E. Marban, Background potassium current active during the plateau of the action potential in guinea pig ventricular myocytes, Circ. Res. 72 (1993) 890–900.
[7] A. Gurney, B. Manoury, Two-pore potassium channels in the cardiovascular system, Eur. Biophys. J. 38 (2009) 305–318.
[8] F. Lesage, C. Terrenoire, G. Romey, M. Lazdunski, Human TREK2, a 2P domain mechano-sensitive K^+ channel with multiple regulations by polyunsaturated fatty acids, lysophospholipids, and Gs, Gi, and Gq protein-coupled receptors, J. Biol. Chem. 275 (2000) 28398–28405.
[9] A.D. Medhurst, G. Rennie, C.G. Chapman, H. Meadows, M.D. Duckworth, R.E. Kelsell, I.I. Gloger, M.N. Pangalos, Distribution analysis of human two pore domain potassium channels in tissues of the central nervous system and periphery, Brain Res. Mol. Brain Res. 86 (2001) 101–114.
[10] W. Gu, G. Schlichthorl, J.R. Hirsch, H. Engels, C. Karschin, A. Karschin, C. Derst, O.K. Steinlein, J. Daut, Expression pattern and functional characteristics of two novel splice variants of the two-pore-domain potassium channel TREK-2, J. Physiol. 539 (2002) 657–668.
[11] W. Liu, D.A. Saint, Heterogeneous expression of tandem-pore K^+ channel genes in adult and embryonic rat heart quantified by real-time polymerase chain reaction, Clin. Exp. Pharmacol. Physiol. 31 (2004) 174–178.
[12] H. Zhang, N. Shepherd, T.L. Creazzo, Temperature-sensitive TREK currents contribute to setting the resting membrane potential in embryonic atrial myocytes, J. Physiol. 586 (2008) 3645–3656.
[13] H. Bang, Y. Kim, D. Kim, TREK-2, a new member of the mechanosensitive tandem-pore K+ channel family, J. Biol. Chem. 275 (2000) 17412–17419.
[14] P.Y. Deng, Z. Xiao, C. Yang, L. Rojanathammanee, L. Grisanti, J. Watt, J.D. Geiger, R. Liu, J.E. Porter, S. Lei, GABA(B) receptor activation inhibits neuronal excitability and spatial learning in the entorhinal cortex by activating TREK-2 K^+ channels, Neuron 63 (2009) 230–243.
[15] D. Kang, C. Choe, D. Kim, Thermosensitivity of the two-pore domain K+ channels TREK-2 and TRAAK, J. Physiol. 564 (2005) 103–116.
[16] G. Sandoz, D. Douguet, F. Chatelain, M. Lazdunski, F. Lesage, Extracellular acidification exerts opposite actions on TREK1 and TREK2 potassium channels via a single conserved histidine residue, Proc. Natl. Acad. Sci. U. S. A. 106 (2009) 14628–14633.
[17] J. Chemin, A. Patel, F. Duprat, M. Zanzouri, M. Lazdunski, E. Honore, Lysophosphatidic acid-operated K+ channels, J. Biol. Chem. 280 (2005) 4415–4421.
[18] J. Chemin, C. Girard, F. Duprat, F. Lesage, G. Romey, M. Lazdunski, Mechanisms underlying excitatory effects of group I metabotropic glutamate receptors via inhibition of 2P domain K^+ channels, EMBO J. 22 (2003) 5403–5411.
[19] D. Kang, J. Han, D. Kim, Mechanism of inhibition of TREK-2 ($K_{2P}10.1$) by the Gq-coupled M3 muscarinic receptor, Am. J. Physiol. Cell Physiol. 291 (2006) C649–C656.
[20] J.T. Shin, M.C. Fishman, From Zebrafish to human: modular medical models, Annu. Rev. Genomics Hum. Genet. 3 (2002) 311–340.
[21] G.J. Lieschke, P.D. Currie, Animal models of human disease: zebrafish swim into view, Nat. Rev. Genet. 8 (2007) 353–367.
[22] I. Skromne, V.E. Prince, Current perspectives in zebrafish reverse genetics: moving forward, Dev. Dyn. 237 (2008) 861–882.
[23] T.P. Barros, W.K. Alderton, H.M. Reynolds, A.G. Roach, S. Berghmans, Zebrafish: an emerging technology for in vivo pharmacological assessment to identify potential safety liabilities in early drug discovery, Br. J. Pharmacol. 154 (2008) 1400–1413.

[24] D.J. Milan, C.A. Macrae, Zebrafish genetic models for arrhythmia, Prog. Biophys. Mol. Biol. 98 (2008) 301–308.
[25] R. Arnaout, T. Ferrer, J. Huisken, K. Spitzer, D.Y. Stainier, M. Tristani-Firouzi, N.C. Chi, Zebrafish model for human long QT syndrome, Proc. Natl. Acad. Sci. U. S. A. 104 (2007) 11316–11321.
[26] D. Hassel, E.P. Scholz, N. Trano, O. Friedrich, S. Just, B. Meder, D.L. Weiss, E. Zitron, S. Marquart, B. Vogel, C.A. Karle, G. Seemann, M.C. Fishman, H.A. Katus, W. Rottbauer, Deficient zebrafish ether-à-go-go-related gene channel gating causes short-QT syndrome in zebrafish reggae mutants, Circulation 117 (2008) 866–875.
[27] L.M. Chen, J. Zhao, R. Musa-Aziz, M.F. Pelletier, I.A. Drummond, W.F. Boron, Cloning and characterization of a zebrafish homologue of human AQP1: a bifunctional water and gas channel, Am. J. Physiol. Regul. Integr. Comp. Physiol. 299 (2010) R1163–R1174.
[28] S.S. Chopra, D.M. Stroud, H. Watanabe, J.S. Bennett, C.G. Burns, K.S. Wells, T. Yang, T.P. Zhong, D.M. Roden, Voltage-gated sodium channels are required for heart development in zebrafish, Circ. Res. 106 (2010) 1342–1350.
[29] D. Panáková, A.A. Werdich, C.A. Macrae, Wnt11 patterns a myocardial electrical gradient through regulation of the L-type Ca(2+) channel, Nature 466 (2010) 874–878.
[30] L. Abbas, S. Hajihashemi, L.F. Stead, G.J. Cooper, T.L. Ware, T.S. Munsey, T.T. Whitfield, S.J. White, Functional and developmental expression of a zebrafish Kir1.1 (ROMK) potassium channel homologue Kcnj1, J. Physiol. 589 (2011) 1489–1503.
[31] R.A. Cornell, Investigations of the in vivo requirements of transient receptor potential ion channels using frog and zebrafish model systems, Adv. Exp. Med. Biol. 704 (2011) 341–357.
[32] M. Kozak, The scanning model for translation: an update, J. Cell Biol. 108 (1989) 229–241.
[33] J. Zhao, L. Hyman, C. Moore, Formation of mRNA 3′ ends in eukaryotes: mechanism, regulation, and interrelationships with other steps in mRNA synthesis, Microbiol. Mol. Biol. Rev. 63 (1999) 405–445.
[34] T. Jowett, L. Lettice, Whole-mount in situ hybridizations on zebrafish embryos using a mixture of digoxigenin- and fluorescein-labelled probes, Trends Genet. 10 (1994) 73–74.
[35] D. Hassel, T. Dahme, J. Erdmann, B. Meder, A. Huge, M. Stoll, S. Just, A. Hess, P. Ehlermann, D. Weichenhan, M. Grimmler, H. Liptau, R. Hetzer, V. Regitz-Zagrosek, C. Fischer, P. Nurnberg, H. Schunkert, H.A. Katus, W. Rottbauer, Nexilin mutations destabilize cardiac Z-disks and lead to dilated cardiomyopathy, Nat. Med. 15 (2009) 1281–1288.
[36] J. Kiehn, D. Thomas, C.A. Karle, W. Schols, W. Kubler, Inhibitory effects of the class III antiarrhythmic drug amiodarone on cloned HERG potassium channels, Naunyn Schmiedebergs Arch. Pharmacol. 359 (1999) 212–219.
[37] M.A. Gates, L. Kim, E.S. Egan, T. Cardozo, H.I. Sirotkin, S.T. Dougan, D. Lashkari, R. Abagyan, A.F. Schier, W.S. Talbot, A genetic linkage map for zebrafish: comparative analysis and localization of genes and expressed sequences, Genome Res. 9 (1999) 334–347.
[38] S.A. Goldstein, L.A. Price, D.N. Rosenthal, M.H. Pausch, ORK1, a potassium-selective leak channel with two pore domains cloned from *Drosophila melanogaster* by expression in *Saccharomyces cerevisiae*, Proc. Natl. Acad. Sci. U. S. A. 93 (1996) 13256–13261.
[39] D. Simkin, E.J. Cavanaugh, D. Kim, Control of the single channel conductance of K_{2P}10.1 (TREK-2) by the amino-terminus: role of alternative translation initiation, J. Physiol. 586 (2008) 5651–5663.
[40] K. Staudacher, I. Baldea, J. Kisselbach, I. Staudacher, A.K. Rahm, P.A. Schweizer, R. Becker, H.A. Katus, D. Thomas, Alternative splicing determines mRNA translation initiation and function of human K_{2P}10.1 K^+ channels, J. Physiol. 589 (2011) 3709–3720.
[41] M. Fink, F. Lesage, F. Duprat, C. Heurteaux, R. Reyes, M. Fosset, M. Lazdunski, A neuronal two P domain K^+ channel stimulated by arachidonic acid and polyunsaturated fatty acids, EMBO J. 17 (1998) 3297–3308.
[42] F. Lesage, R. Reyes, M. Fink, F. Duprat, E. Guillemare, M. Lazdunski, Dimerization of TWIK-1 K^+ channel subunits via a disulfide bridge, EMBO J. 15 (1996) 6400–6407.
[43] Y. Kim, C. Gnatenco, H. Bang, D. Kim, Localization of TREK-2 K^+ channel domains that regulate channel kinetics and sensitivity to pressure, fatty acids and pHi, Pflugers Arch. 442 (2001) 952–960.
[44] D. Kim, Fatty acid-sensitive two-pore domain K^+ channels, Trends Pharmacol. Sci. 24 (2003) 648–654.
[45] J. Gierten, E. Ficker, R. Bloehs, P.A. Schweizer, E. Zitron, E. Scholz, C. Karle, H.A. Katus, D. Thomas, The human cardiac K_{2P}3.1 (TASK-1) potassium leak channel is a molecular target for the class III antiarrhythmic drug amiodarone, Naunyn Schmiedebergs Arch. Pharmacol. 381 (2010) 261–270.
[46] C.E. Clarke, E.L. Veale, P.J. Green, H.J. Meadows, A. Mathie, Selective block of the human 2-P domain potassium channel, TASK-3, and the native leak potassium current, IKSO, by zinc, J. Physiol. 560 (2004) 51–62.
[47] M. Gruss, A. Mathie, W.R. Lieb, N.P. Franks, The two-pore-domain K(+) channels TREK-1 and TASK-3 are differentially modulated by copper and zinc, Mol. Pharmacol. 66 (2004) 530–537.
[48] J.S. Kim, J.Y. Park, H.W. Kang, E.J. Lee, H. Bang, J.H. Lee, Zinc activates TREK-2 potassium channel activity, J. Pharmacol. Exp. Ther. 314 (2005) 618–625.
[49] I.G. Woods, P.D. Kelly, F. Chu, P. Ngo-Hazelett, Y.L. Yan, H. Huang, J.H. Postlethwait, W.S. Talbot, A comparative map of the zebrafish genome, Genome Res. 10 (2000) 1903–1914.
[50] J.S. Taylor, I. Braasch, T. Frickey, A. Meyer, Y. Van de Peer, Genome duplication, a trait shared by 22000 species of ray-finned fish, Genome Res. 13 (2003) 382–390.
[51] J.H. Postlethwait, I.G. Woods, P. Ngo-Hazelett, Y.L. Yan, P.D. Kelly, F. Chu, H. Huang, A. Hill-Force, W.S. Talbot, Zebrafish comparative genomics and the origins of vertebrate chromosomes, Genome Res. 10 (2000) 1890–1902.
[52] W.B. Barbazuk, I. Korf, C. Kadavi, J. Heyen, S. Tate, E. Wun, J.A. Bedell, J.D. McPherson, S.L. Johnson, The syntenic relationship of the zebrafish and human genomes, Genome Res. 10 (2000) 1351–1358.
[53] I.G. Woods, C. Wilson, B. Friedlander, P. Chang, D.K. Reyes, R. Nix, P.D. Kelly, F. Chu, J.H. Postlethwait, W.S. Talbot, The zebrafish gene map defines ancestral vertebrate chromosomes, Genome Res. 15 (2005) 1307–1314.
[54] K. Staudacher, I. Staudacher, E. Ficker, C. Seyler, J. Gierten, J. Kisselbach, A.K. Rahm, K. Trappe, P.A. Schweizer, R. Becker, H.A. Katus, D. Thomas, Carvedilol targets human K_{2P}3.1 (TASK1) K^+ leak channels, Br. J. Pharmacol. 163 (2011) 1099–1110.
[55] D.J. Milan, T.A. Peterson, J.N. Ruskin, R.T. Peterson, C.A. MacRae, Drugs that induce repolarization abnormalities cause bradycardia in zebrafish, Circulation 107 (2003) 1355–1358.